# Low-frequency geoid modelling based on 3D mass optimisation

**J. J. Fellner*, M. Kuhn, W. E. Featherstone**

**This paper demonstrates an iterative optimisation algorithm, where a pre-defined low-frequency geoid model is simulated based on assumptions about mass-density distributions within the upper mantle. This aims to model low-frequency spectra of the anomalous external Earth's gravity field to produce a realistic synthetic Earth gravity model (SEGM). All mass anomalies are represented by an envelope of 3D discrete bodies (prisms) that refer to a regular geographic grid on a spherical reference surface. The optimisation algorithm uses forward gravity field modelling techniques based on Newton's integral to derive the gravitational potential of each 3D mass element, and subsequently its effect on the synthetic (simulated) geoid height via Bruns's formula. Geoid height differences from a given reference model (EGM2008) are minimised by applying the mass-model optimisation algorithm that iteratively modifies the volume (prism height) of each mass element introduced. Finally, the effectiveness of the optimisation algorithm is demonstrated through a numerical example for regional-scale geoid modelling over Austria. A mass-model was created that inversely produces a similar pattern compared to the observed gravity field given by EGM20008 where the differences are within several centimetres of the geoid height.**

## 1 Introduction

Forward gravity-field modelling has become a more prominent geodetic topic, as simulations of the Earth's external gravity field – so-called Synthetic Earth Gravity Models (SEGMs) – offer the opportunity to validate gravity-field-related algorithms, theories, techniques and any related computer software (e.g., Featherstone 1999, Kuhn and Featherstone 2005, Baran et al. 2006, Tsoulis and Kuhn 2007). The advantage of a SEGM is that the derived gravity field quantities are self-consistent within the pre-defined model assumptions, such as with respect to a simulated mass distribution. Forward gravity field modelling has become more attractive principally because of the availability of high-performance computer facilities. Van Gelderen (1991) generated a relatively simple 2D SEGM, which showed that even a 2D synthetic world can contribute to a better understanding of some aspects of physical geodesy. Nowadays and thanks to supercomputers, we are able to deal with far more complicated 3D models based on higher resolution and more accurate local, regional and global data sets. Due to a global data pool of public-domain and networked databases, the user can easily decide how sophisticated and/or realistic the Earth's gravity field can be replicated by a SEGM.

A niche of the geodetic community has constructed SEGMs on local, regional and global scales for various applications (e.g., Barthelmes and Dietrich 1991, Vermeer 1995, Pail 1999, Haagmans 2000, Kuhn and Featherstone 2005, Baran et al. 2006). Generally, there are two different approaches to create a SEGM (e.g. Pail 1999); either using a *source model* or an *effect model*. In general, source models assume a mass-density distribution within the solid Earth and apply forward gravity modelling techniques (e.g., Kuhn 2003, Kuhn and Featherstone 2005). Effect models follow an opposite approach without any pre-defined assumptions of masses within the Earth (e.g., Tziavos 1996, Haagmans 2000, Claessens 2002). Instead they are based on external observations of the Earth gravity field usually combined in an Earth Gravity Model (EGM). Both options are in common use and have been successfully applied in geodetic studies. Another possibility to construct a SEGM is to combine source and effect models in so-called *hybrid source-effect models*. These models combine the advantage of the effect model – considering the long-wavelength structure from the global gravity model – with the advantage of the source model – the high-frequency impact of near and high-resolution surface mass-density distributions (e.g., Baran et al. 2006).

In order to create a realistic simulation of the Earth's gravity field, there is a tendency to use already known (global) information about the real Earth instead of making vague and unrealistic model assumptions. In doing so, however, it is neglected that even additional unrealistic mass model assumptions may lead to further SEGM improvements. This is even more important considering that currently available information on the Earth's topography, bathymetry, crust and mantle seem to be insufficient for reconstructing the global anomalous gravity field signal, with some differences in the geoid height being more than twice as large as the signal range itself (Kuhn and Featherstone 2005, Fellner et al. submitted).

The aim of a SEGM is to reproduce gravity field-related parameters as-realistically-as-possible, whether the model assumptions used are close to reality or not. While the former will increase the acceptance of a SEGM, the latter is permissible as long as the SEGM is used only in its definition space; the space where it reproduces realistic gravity field-related parameters. Here we explore the effect of one particular mass element (prism) on the simulated geoid height and how this information can be used in an iterative mass-model optimisation algorithm.

In the remainder of this article, we associate a particular mass element to a right rectangular prism with flat top and flat bottom, but acknowledge that other geometries can be employed. We demonstrate the ability of our developed algorithm to adjust regional mass distributions that simulate the Earth's anomalous gravity field signal. Here we specifically focus on the lower frequency constituents and demonstrate the potential of the optimisation algorithm to improve the low-frequency spectra of a SEGM by applying it to regional-scale geoid modelling over Austria.

## 2 The influence of single mass elements on the synthetic geoid height

Since each mass element within the solid Earth has an effect on the external geopotential, and that no significant knowledge about the mass-density distribution of deeper-seated masses within the lower mantle is currently available, it is necessary to assume masses at user-defined locations when following the synthetic approach. Here we start with some elementary considerations on the effect of single mass elements on the simulated geoid height before presenting our iterative optimisation algorithm in more detail.

Figure 1 shows one particular mass element at a user-defined surface at depth $d$ below a reference surface (e.g., reference sphere or ellipsoid on a global scale). Here we assume the mass element to be centred over the particular grid point $P_{ij}$ of a regular geographic grid where the subindices $i = 1 \ldots lat\_max$ and $j = 1 \ldots lon\_max$ indicate a specific grid element.

Based on Newton's law of gravitation, the effect on the gravitational potential $\delta V(Q_{ij})$ at the location $Q_{ij}$ on the reference surface induced by a single prism located at $P_{ij}$ is given by (e.g., MADER 1955, NAGY et al. 2000, 2002)

$$\delta V(Q_{ij}) = \delta V_{ij} = G \cdot \rho_{ij} \cdot u(P_{ij}, Q_{ij}) \tag{1}$$

where

$$u(P_{ij}, Q_{ij}) = \int_v \frac{dv}{l(P_{ij}, Q_{ij})} = \int_x \int_y \int_z \frac{dxdydz}{l(P_{ij}, Q_{ij})} \tag{2}$$

is the (triple) volume integral over the body $v$ of the prism, $\rho_{ij}$ it the constant mass-density, $l(P_{ij}, Q_{ij})$ is the Euclidian distance between the computation point $Q_{ij}$ and the mass element located at $P_{ij}$ and $G$ indicates Newton's gravitational constant. For more details on the explicit formulas, the interested reader is referred to MADER (1955) and NAGY et al. (2000, 2002). Using Bruns's formula (e.g., HEISKANEN and MORITZ 1967), the effect on the gravitational potential $\delta V_{ij}$ can be converted into the effect on the synthetic geoid height

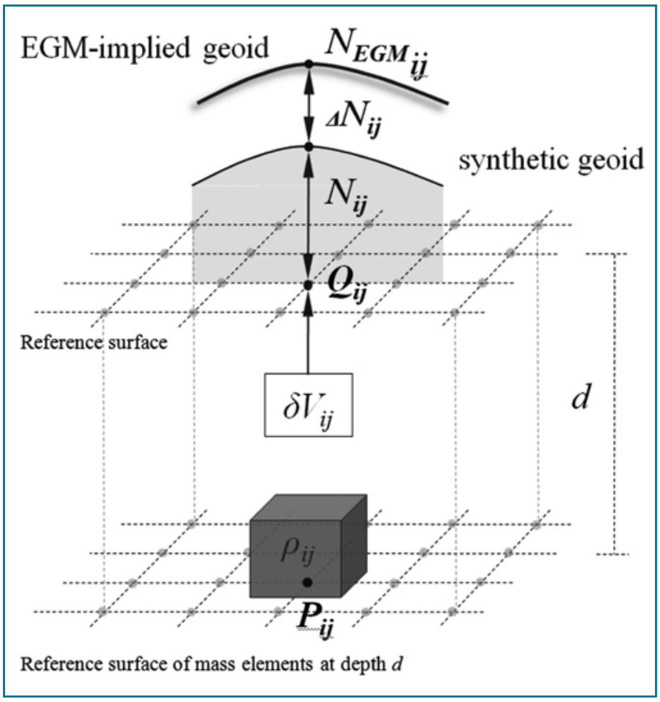


*Fig. 1: Geometric relation between a particular mass element at the grid point $P_{ij}$ at a user-defined depth d and its effect on the synthetic geoid height $\delta N_{ij}$ at the same horizontal grid location. Both the geoid height and the depth of the mass element are measured from the same reference surface (e.g. a reference sphere or ellipsoid)*

$$\delta N(Q_{ij}) = \delta N_{ij} = \frac{\delta V_{ij}}{\gamma_{ij}} \tag{3}$$

where $\gamma$ is the latitude-dependent normal gravity on the surface of the used reference gravity model (e.g., on the surface of the GRS80 reference ellipsoid). Finally, the superposition of all mass element effects provides the synthetic geoid height at location $Q_{ij}$ by

$$N(Q_{ij}) = N_{ij} = \sum_{ij} \delta N_{ij}. \tag{4}$$

The quality of the synthetic geoid height can be evaluated through comparison with an EGM expressed by the differences

$$\Delta N_{ij} = N_{EGMij} - N_{ij}. \tag{5}$$

where the EGM has been evaluated through spherical harmonic synthesis at the same grid locations $Q_{ij}$.

For the practical evaluation of equation (1), it is necessary to define the depth $d$ of the mass elements, as well as their dimensions and total mass. The latter are described by the prism base surface, height and a constant mass-density. As will be described in the next section, we will fix the depth $d$, the constant mass density $\rho_{ij}$ and indirectly the base surface through the grid resolution used, and thus only adjust the height (or volume) of the prism. Our calculations of the gravitational potential (cf. equation 1) are based on the principles described in KUHN (2000, 2003), where the gravitational effect of an elliptical (or spherical) mass element is evaluated by that of a mass equal prism of the same height and centred at the same horizontal location.

As an aside, the assumed depth $d$ of the mass elements can be chosen dependent on the frequency bandwidth of the geoid height that the user wants to approximate. Following the formula of Bowin (1983), it is possible to determine the minimum depth $d_n$ of a mass element through

$$d_n = \frac{R}{n-1}. \tag{6}$$

where the spectral content of the geoid height to be modelled is expressed by the spherical harmonic degree $n$. According to equation (6), geoid contributions, dependent on an individual degree $n$, have a fixed ratio value in proportion to that of assumed masses at a depth $d_n$ of some fraction of the Earth radius $R$.

Finally, it is important to acknowledge that a constant depth for all mass elements provides significant computational advantage through a much faster evaluation of equation 2, but this is not an essential requirement.

## 3 An iterative mass-model optimisation algorithm

Based on the elementary relations presented in the previous section, we now present an iterative mass-model optimisation algorithm by evaluating the geoid height differences $\Delta N_{ij}$ introduced by equation (5). Here we assume that the synthetic geoid heights at the locations $Q_{ij}$ are co-located with the grid locations $P_{ij}$ of the mass elements, thus there are as many geoid height differences as mass elements (cf. Figure 1). Depending on the sign and magnitude of the geoid height difference $\Delta N_{ij}$, it is possible to provide a simple assessment of the underling (simulated) mass-model as the synthetic geoid heights directly depend on it (cf. equation 3).

Assuming that only the mass element at the location $P_{ij}$ is responsible for the signal in $\Delta N_{ij}$, then a positive difference indicates mass deficiencies of the corresponding mass element, whereas a negative difference indicates mass excess. We account for the mass deficiencies/excess by adjusting the corresponding prism height to a greater/smaller value, respectively. Furthermore, based on the magnitude of $\Delta N_{ij}$, a strategy can be devised in order to derive the amount of change in the prism height (see step 4 of the iterative procedure below). While this adjustment strategy is rather simple, it completely neglects the effect of neighbouring mass elements (theoretically all other mass elements), thus further adjustments have to be made. Below we provide a step-by-step description for an iterative adjustment procedure that accounts for this shortcoming.

**STEP 1:** In order to start the iterative procedure, initial values for the heights of each mass-prism have to be defined. If no prior information is available, the initial heights can be set to zero, thus the iteration starts with zero additional masses. Furthermore, the (constant) depth $d$ and the constant mass density $\rho_{ij}$ for all prisms have to be defined. The size of the base surfaces of the prisms are provided indirectly by way of the grid resolution used.

**STEP 2:** Based on the initial values defined in step 1, the effect on the synthetic geoid is derived through the evaluation of equation (4). This is the most time-consuming part of the procedure because equation (2) has to be evaluated for all combinations between computation points and mass elements. For example, for a grid with *lat_max* by *lon_max* elements, equation (2) has to be evaluated $(lat\_max \times lon\_max)^2$ times. Some improvements that reduce the computational effort can be introduced, such as the use of coarser resolution prism and mass bodies of simpler geometry (e.g., point masses) for more distant masses with respect to the computation point (cf. Kuhn 2000, 2003).

**STEP 3:** The synthetic geoid height resulting from step 2 is used to derive the geoid height differences with respect to the EGM (cf. equation 5). The magnitudes of the differences provide information on the closeness of the SEGM to the 'observed' EGM. This implicitly assumes that the EGM is error-free, which is an acceptable assumption in the construction of a SEGM. Based on the geoid height differences (a convergence criterion), the decision is made if a further improvement of the simulated mass model (e.g., the prism heights or mass-density) is required. Here we use the overall RMS value (RMS-fit) of the differences and compare it to a pre-defined threshold. If unsatisfactory, the prism heights will be adjusted further in step 4, otherwise the iteration will be stopped.

**STEP 4:** Adjust the prism heights used in step 2 based on the sign and magnitude of the geoid height differences obtained in step 3. The adjustment is done by an incremental change $\delta h_{ij}$ of the corresponding prism heights. The incremental change can be either a constant value or dependent on the magnitude of the geoid height differences. The latter is more sensible as it gives optimisation preference to areas exhibiting larger differences. Here we apply a predefined increment $\delta h_{ij}$ only if the geoid height is larger than a given threshold. Finally, we introduce an increment that is variable with the number of iteration steps in the way that larger increments are used at the early stages of the iteration and smaller increments at later stages (cf. Table 1 in section 4). Test calculations have revealed that this is a simple but very effective way to dramatically reduce the number of iterations steps. After all prism heights have been adjusted, repeat steps 2 and 3 as long as the RMS-fit is larger then the given threshold (cf. step 2).

The iterative mass-model optimisation algorithm described above has been implemented in a FORTRAN95 program. In order to run the program, the user has to define the following settings that will have major influence on the structure of the final mass-model as well as the convergence behaviour of the iterations:

- Depths of the mass elements considered. Currently, all mass elements are considered at the same constant depth. According to equation (6), the user can control what frequency band-width will be modelled.
- Constant mass-density of all prisms used. Together with the depth information, the user can replicate geophysical information, such as the average depths and mass-density of an anomalous mass distribution.

– Horizontal extension of the prisms, which is defined indirectly through the selection of the grid resolution. Kuhn and FKeatherstone (2003) provide some information on the optimum spatial resolution required to model the geoid height to a pre-defined precision level.
– Maximum number of iteration steps. This setting is very important in test or validation calculations when an inappropriate height increment has been selected (e.g., the convergence can be rather slow if this has been set inappropriately).
– Criteria to stop the iteration (see step 3 of the iterative procedure). As mentioned above, here a threshold can be defined for the overall RMS-fit of the synthetic model to the EGM.
– Threshold used for a particular geoid height difference to decide if the corresponding prism height will be adjusted (see step 4 of the iterative procedure).
– Height increment used to improve the prism heights in each iteration step. The user can decide what increment value is used at each particular iteration step or interval of iteration steps (see step 4 of the iterative procedure).

Finally, it is important to mention that similar optimisation algorithms could be developed that do not change the height of each prism. For example, a fixed height could be introduced for each prism (constant or variable with location) and their mass-densities could be adjusted. This leads to a lateral variable mass-density distribution. Such a strategy would be useful when prior information on the geometry of an anomalous mass distribution is known (e.g., one of the major discontinuities in the upper mantle). Alternatively, keeping size and mass-density fixed, the location (i.e., depth) of each prism can be adjusted.

Furthermore, the mass body used can be changed. For example, due to rather simple mathematical relations, the fit of a set of point masses is frequently done in gravity field modelling (e.g., Barthelmes and Dietrich 1991, Claessens et al. 2001, Vermeer, 1995). However, when constructing a SEGM, the kind of optimisation used is of secondary importance as long as the SEGM produces a realistic representation of the Earth's gravity field. The kind of optimisation may become important for the convergence behaviour, which however needs to be investigated further. Instead, we focus on the iterative optimisation algorithm only, but acknowledge other algorithmic possibilities.

## 4 Modelling the low-frequency geoid over Austria

In order to demonstrate the effectiveness of the developed mass-model optimisation algorithm, we apply it to regional-scale geoid modelling over Austria. We focus on the low-frequency bandwidth with wavelengths of few hundred kilometres, corresponding to a maximum spherical harmonic degree of $N = 90$. To validate the synthetic geoid, EGM2008 (Pavlis et al. 2008) was used up to degree and order $N = 90$ and evaluated on a 0.1° by 0.1° geographic grid over the area bounded by 9 °E – 18 °E and 46 °N – 50° (cf. Figure 2). This has been done using the harmonic synthesis routine provided by the EGM2008 Development Team (EGM 2008). The higher than Nyquist grid resolution has been cho-

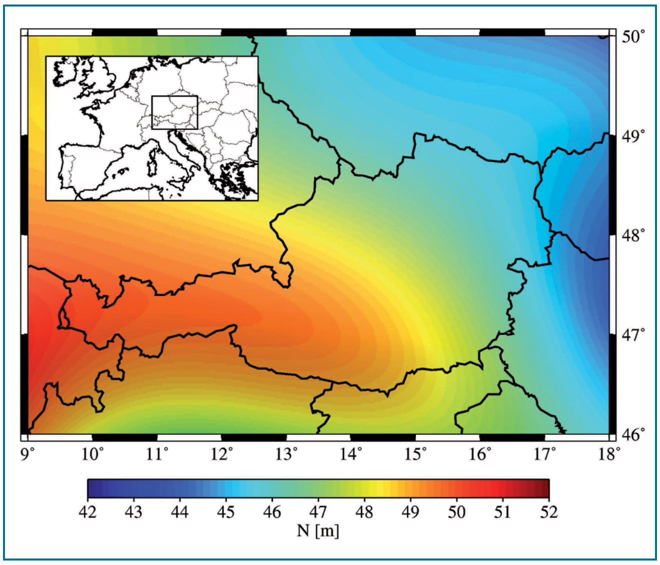


*Fig. 2: The EGM2008-implied low-frequency geoid over Austria developed up to degree and order $N = 90$. (units in metres; Mercator projection)*

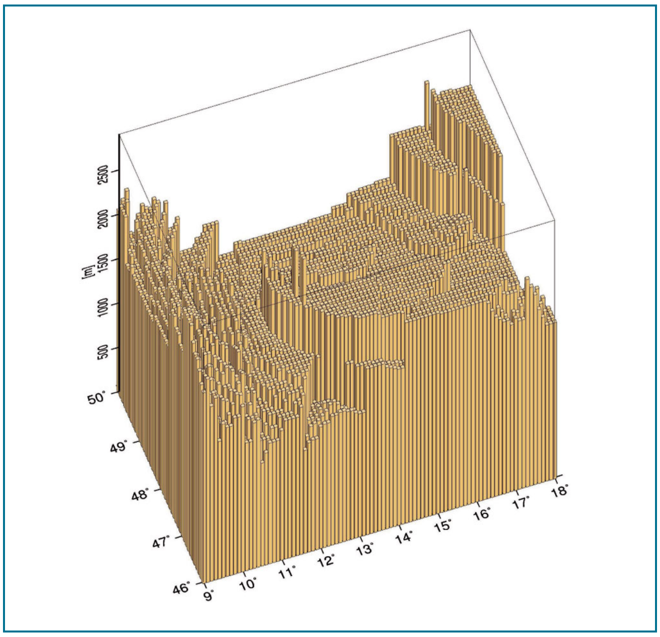


*Fig. 3: 3-D plot of the final mass model assumed at a reference depth of 33 kilometres showing all prisms (units in metres).*

sen in order to avoid unrealistically large step-functions (large height changes) between neighbouring prisms of the SEGM.

Based on the relation provided by Bowin (1983) (cf. equation 6) we use a constant depth for the prisms of 33 km, which is appropriate to model spectral constituents up to a spherical harmonic degree of $N = 192$. This corresponds to approximately twice the spectral content as represented by $N = 90$, which should be more then sufficient to model regional-scale geoid heights. In addition, the depth of 33 km corresponds approximately to an average depth of the Mohorovičić discontinuity (Moho) over the area considered (e.g., see Figure 6 in Abd-Elmotaal and Kühtreiber 2003). The anomalous masses have been assigned with a constant mass-density anomaly of $\Delta\rho = 1000$ kgm$^{-3}$, which is a valid assumption within the synthetic approach, as it is not the aim to create a realistic subsurface mass model, but rather to simulate as closely as possible the geoid heights provided by EGM2008 (cf. Figure 2).

For the selected low-frequency spectrum, the observed geoid height values implied by EGM2008 over Austria range between + 43.7 m and + 50.5 m, with a mean value of + 47.4 m. The spatial pattern is characterised by an increase of the geoid height from East to West with minimum values over the flatter areas in the North-East (e.g., the Vienna basin) and maximum values in the West representing the mountainous area of the Austrian Alps. Therefore, the spatial pattern shows some general correlation with the underlying topography, which is consistent with gravimetric geoid modelling results over this area (Abd-Elmotaal and Kühtreiber 2003).

An optimised mass-model over Austria was obtained by the application of the developed iterative optimisation algorithm (cf. Figure 3). It was obtained after 202 iteration steps when the RMS-fit fell below the pre-set threshold of 5 cm. The number of iteration steps, height increments used and convergence behaviour are outlined in Table 1.

The processing time was about seven hours using the iVec supercomputing facilities (www.ivec.org) with the following specifications (host type: SGI Altix XE 1300, 512 CPUs, 1TB RAM).

The final mass-model is illustrated in Figure 3, showing the envelope surface given by all prisms on the regular geographic grid of 0.1 ° by 0.1 ° resolution. The prism heights range between 540 m and 2850 m, with an average height of 1679 m. The spatial distribution of the prism heights neither correlates with the spatial pattern of the geoid height nor the topography over Austria. This is an effect of the mutual interaction of all mass elements that produce the final geoid height. That is, there is not a one-to-one correlation between the mass layer and the Austrian geoid because the topography is handled separately from the optimised 33 km-depth mass layer.

Finally, the synthetic geoid obtained from forward gravity modelling the optimised mass model is illustrated in Figure 4, showing the same spatial pattern then that of EGM2008 (cf. Figure 2). This demonstrates the effectiveness of the developed mass model optimisation algorithm. The differences, representing model errors, are displayed

*Table 1: Layout of the optimisation and convergence behaviour expressed by the overall RMS-fit*

| Iteration Steps | Height increment $\delta h_{ij}$ [m] | RMS-fit [m] |
|---|---|---|
| 1–8 | 500 | 3.41 |
| 9–78 | 100 | 0.78 |
| 79–128 | 50 | 0.41 |
| 129–178 | 20 | 0.16 |
| 179–202 | 10 | 0.05 |
| *processing time: 07 h:11 m:17 sec (iVec/XE)* | | |

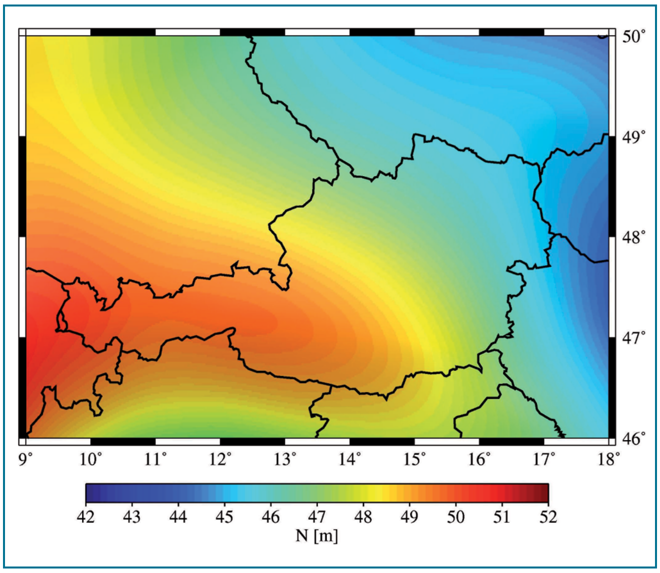


*Fig. 4: Synthetic geoid obtained by forward gravity modelling of the optimised mass model (units in metres; Mercator projection)*

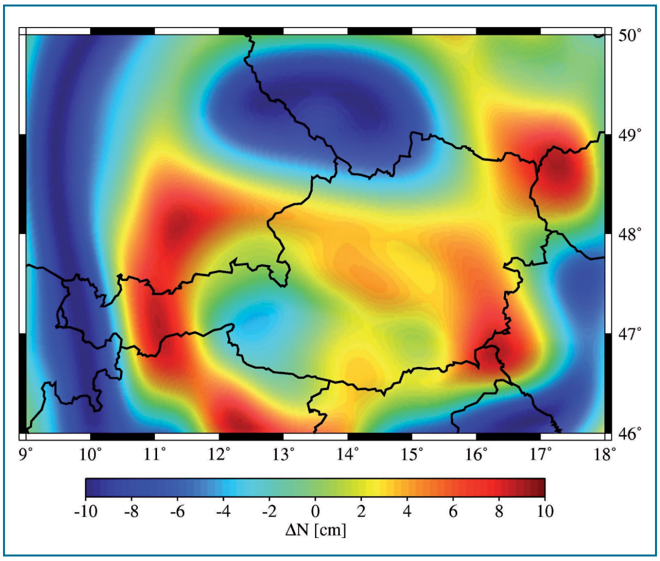


*Fig. 5: Differences between the EGM2008 and synthetic geoid height. (units in centimetres; Mercator projection)*

in Figure 5 ranging between − 10 cm and + 9 cm with an RMS value of ± 5 cm, as specified by the convergence criterion. Like the mass model, the spatial pattern of the differences neither correlates with the geoid heights nor the topography over Austria.

## 5 Conclusions

This paper has presented a new way of modelling the low-frequency geoid spectrum based on forward gravity modelling an optimised mass model at the crust-mantle boundary. Test calculations over Austria have shown that the developed approach is able to provide a mass model that is consistent with the observed low-frequency gravity field expressed here by the geoid height. Differences between the synthetic (simulated) geoid and that implied by EGM2008 are below 10 cm with an RMS value of ± 5.0 cm, as was specified in the optimisation loop.
The modelling is based on an iterative mass model optimisation algorithm that fits a set of prisms so to provide minimum differences when comparing the induced gravitational potential with that of an EGM. The core of the algorithm is based on forward gravity modelling in the space domain, thus the direct application of Newton's integral on the simulated mass model. As shown over Austria, the use of 3D mass elements (prisms) allows for the development of mass distributions with an almost arbitrary geometry. This is an advantage of using prisms compared to mass bodies of simpler geometry (e.g., point masses or surface mass elements). However, due to the more complex computation formulas, the use of prisms is limited when considering high-resolution applications over large areas as the computation time will become the major issue.
While the developed algorithm has been tested for low-frequency geoid modelling on a region-scale, it can be equally applied to any frequency band-width, as well as to any computation region (e.g., local, regional and global). Furthermore, the same procedure can be used with other more or less complex mass bodies. Once again, the limitations will be given by the computation power available. However, with the increased availability of supercomputers, the boundary can be pushed to more complex applications.
Finally, it should be mentioned again that the resultant mass model may be far from reality, thus any geophysical interpretation of it has to be handled with extreme care, considering all assumptions made. This is certainly the fact when only one major mass source is used (e.g. one mass layer at the crust-mantle boundary) as, in this case, all other existing mass anomalies will be accounted for in this mass source. However, this is not a problem when constructing a SEGM as it is not to be used for geophysical interpretation. In order to improve the mass model further, the developed procedure can be applied to an arbitrary number of mass sources (e.g., multiple mass layers), thus it offers the possibility to incorporate other geophysical information on the Earth's interior.

Acknowledgements. *We would like to thank the EGM2008 Development Team for providing the harmonic_synth_v2.f software, which allowed calculation of the low-frequency reference geoid over Austria. This work was supported by iVEC through the use of advanced computing resources provided by the ARRC facility located at Technology Park, Perth, Western Australia. JJF and MK acknowledge funding from Curtin University's Institute for Geoscience Research (TIGeR). MK wishes to thank Curtin University of Technology for support within his Research and Teaching Fellowship. WEF receives funding support under the Australian Research Council's discovery projects funding scheme (grant DP0663020). We would also like to thank the reviewers for their time taken to assess this manuscript. This is TIGeR publication number 217.*

## References


[1] Abd-Elmotal, H. A.; Kühtreiber, N. (2003): Geoid determination using adapted reference field, seismic Moho depths and variable density contrast. Journal of Geodesy, 77: 77–85

[2] Baran, I.; Kuhn, M.; Claessens, S. J.; Featherstone, W. E.; Holmes, S. A.; Vanícek, P. (2006): A synthetic Earth gravity model designed specifically for testing regional gravimetric geoid determination algorithms. Journal of Geodesy 80(1):1–16, doi: 10.1007/s00190-005-0002-z

[3] Bowin, C. (1983): Depth of principal mass anomalies contributing to Earth's geoid undulations and gravity anomalies. Marine Geodesy 7, 61–100

[4] Barthelmes, F.; Dietrich, R. (1991): Use of Point Masses on Optimized Positions for the Approximation of the Gravity Field. In R. H. Rapp and F. Sanso (Eds.), Determination of the Geoid: Present and Future, Springer, Berlin, pp 484

[5] Claessens, S. J. (2002): A synthetic Earth model analysis, implementation, validation and application. MSc. thesis, Delft University of Technology, Delft, Netherlands

[6] EGM (2008): Earth Gravitational Model 2008. U.S. National Geospatial-Intelligence Agency (NGA), Team http://earthinfo.nga.mil/GandG/wgs84/gravitymod/egm2008/index.htm l

[7] Featherstone, W. E. (1999): Progress report for IAG SSG3.177 Synthetic Modelling of the Earth's Gravity Field, in: Anderson, O.B. (ed) International Association of Geodesy Travaux http://www.gfy.ku.dk/~iag/Travaux/ssg3177.htm

[8] Fellner, J. J.; Kuhn, M.; Featherstone, W. E. (submitted): Development of a Synthetic Earth Gravity Model by 3D mass optimisation based on forward gravity modelling. Earth and Planetary Science

[9] Haagmans, R. (2000): A synthetic Earth for use in geodesy. Journal of Geodesy 74 (7–8): 503–511

[10] Heck, B.; Seitz, K. (2006): A comparison of the tesseroid, prism and pointmass approaches for mass reductions in gravity field modelling. Journal of Geodesy 81 (2): 121–136

[11] Heiskanen, W.; Moritz, H. (1967): Physical geodesy. WH Freeman & Co, San Francisco

[12] Kuhn, M. (2000): Geoidbestimmung unter Verwendung verschiedener Dichtehypothesen. Deutsche Geodätische Kommission, Reihe C, No. 520, München, Germany, 128pp

[13] Kuhn, M. (2003): Geoid determination with density hypothesis from isostatic models and geological information. Journal of Geodesy 77(1–2): 50–65

[14] Kuhn, M.; Featherstone, W. E. (2003): On the optimal spatial resolution of crustal mass distributions for forward gravity field modelling. In Tziavos IN (ed) Gravity and Geoid 2002, Proceedings of the 3rd meeting of the International Gravity and Geoid Commission, Thessaloniki, Greece, 195–200

[15] Kuhn, M.; Featherstone, W. E. (2005): Construction of a synthetic Earth Gravity Model by Forward Gravity Modelling. In A Window on the Future of Geodesy, Volume 128 of International Association of Geodesy Symposia, pp 350–355. Springer Berlin Heidelberg

[16] Mader, K. (1951): Das Newtonsche Raumpotential prismatischer Körper und seine Ableitungen bis zur dritten Ordnung. Österreichische Zeitschrift für Vermessungswesen, Sonderheft 11

[17] Nagy, D. (1966): The gravitational attraction of a right rectangular prism. Geophysics 31 (2): 362–371

[18] Nagy, D.; Papp, G.; Benedek, J. (2000): The gravitational potential and its derivatives for the prism. Journal of Geodesy 74: 522–560

[19] Nagy, D.; Papp, G.; Benedek, J. (2002): Corrections to "The gravitational potential and its derivatives for the prism". Journal of Geodesy 76, 475

[20] Pail, R. (1999): Synthetic global gravity model for planetary bodies and applications in satellite gradiometry. Ph.D. thesis, Technical University of Graz, Graz, Austria

[21] Pavlis, N. K.; Holmes, S. A.; Kenyon, S. C.; Factor, J. K. (2008): An Earth gravitational model to degree 2160: EGM2008. Presented at the 2008 General Assembly of the European Geosciences Union, Vienna, Austria, April 13–18 2008

[22] Tsoulis, D.; Kuhn, M. (2007): Recent developments in synthetic Earth gravity models in view of the availability of digital terrain and crustal databases of global coverage and increased resolution. In A. Kiliçoğlu, R. Forsberg (eds.): Gravity Field of the Earth, Proceedings of the 1st International Symposium of the IGFS, Harita Dergisi, Ankara, Turkey, 354–359

[23] Tziavos, I. (1996): Comparison of spectral techniques for geoid computations over large regions. Journal of Geodesy 70 (6): 357–373

[24] Van Gelderen, M. (1991): The geodetic boundary value problem in two dimensions and its iterative solution. Publ 35, Netherlands Geodetic Commission, Delft

[25] Vermeer, M. (1995): Mass point geopotential modelling using fast spectral techniques; historical overview, toolbox description, numerical experiment. Manuscr Geod 20(5): 362–378



Adresses of the authors:

J.J. Fellner*, M. Kuhn, W.E. Featherstone, Western Australian Centre for Geodesy & The Institute for Geoscience Research, Curtin University of Technology, GPO Box U1987, Perth, WA 6845, Australia;

* fax + 61-8-92 66-27 03; email: fellnerjf@yahoo.com.au